

ARTICLE

Received 16 May 2016 | Accepted 28 Dec 2016 | Published 8 Feb 2017

DOI: 10.1038/ncomms14422

OPEN

LncRNA AK023948 is a positive regulator of AKT

Pratirodh Koirala^{1,2}, Jianguo Huang^{1,2}, Tsui-Ting Ho^{1,3,4}, Fangting Wu⁵, Xianfeng Ding^{1,6} & Yin-Yuan Mo^{1,3}

Despite the overwhelming number of human long non-coding RNAs (lncRNAs) reported so far, little is known about their physiological functions for the majority of them. The present study uses a CRISPR/Cas9-based synergistic activation mediator (SAM) system to identify potential lncRNAs capable of regulating AKT activity. Among lncRNAs identified from this screen, we demonstrate that AK023948 is a positive regulator for AKT. Knockout of AK023948 suppresses, whereas rescue with AK023948 restores the AKT activity. Mechanistically, AK023948 functionally interacts with DHX9 and p85. Importantly, AK023948 is required for the interaction between DHX9 and p85 to hence the p85 stability and promote AKT activity. Finally, AK023948 is upregulated in breast cancer; interrogation of TCGA data set indicates that upregulation of DHX9 in breast cancer is associated with poor survival. Together, this study demonstrates two previously uncharacterized factors AK023948 and DHX9 as important players in the AKT pathway, and that their upregulation may contribute to breast tumour progression.

¹Cancer Institute, University of Mississippi Medical Center, Jackson, Mississippi 39216, USA. ²Department of Biochemistry, University of Mississippi Medical Center, Jackson, Mississippi 39216, USA. ³Department of Pharmacology/Toxicology, University of Mississippi Medical Center, Jackson, Mississippi 39216, USA. ⁴Department of Radiation Oncology, University of Mississippi Medical Center, Jackson, Mississippi 39216, USA. ⁵System Biosciences, Mountain View, California 94041, USA. ⁶College of Life Sciences, Zhejiang Sci-Tech University, Hangzhou 310022, China. Correspondence and requests for materials should be addressed to X.D. (email: bdd114@163.com) or to Y.M. (email: ymo@umc.edu).

Advances in functional genomics have revealed that the human genome is actively transcribed; however, vast majority of the transcripts are non-coding RNA including microRNAs and long non-coding RNAs (lncRNAs)¹. Unlike microRNAs, lncRNAs are larger than 200 bp in length, and some of them may be capped and polyadenylated. Increasing evidence suggests that lncRNAs could be the key regulators of different cellular processes. Various mechanisms have been proposed to explain how lncRNAs may have an impact on gene expression. One of well-characterized mechanisms is the lncRNA-mediated gene regulation through interaction with DNA, RNA or protein. For instance, HOTAIR acts as a scaffold to recruit proteins required for chromatin remodelling². On the other hand, GAS5 imitates glucocorticoid response element and binds to glucocorticoid receptor such that it prevents from binding to its response element³. In addition, GAS5 inhibits the expression of miR-21 through the competing endogenous RNA mechanism⁴. There are many other examples of lncRNAs as scaffolds that bring together multiple proteins to form functional ribonucleoprotein complexes^{5–8}. Through interactions with different binding partners, lncRNAs can regulate their function, stability or activity.

The phosphoinositide-3-kinase (PI3K)–protein kinase B/AKT (PI3K-PKB/AKT) pathway is at the centre of cell signalling; it responds to growth factors, cytokines and other cellular stimuli. Once activated, AKT transfers signaling and regulates an array of downstream targets including well-known MDM2/p53, Foxo and NF- κ B. As a result, AKT plays a key role in the diverse cellular processes, including cell survival, growth, proliferation, angiogenesis, metabolism and cell migration⁹. The AKT activity can be influenced by many factors, such as growth factors or their corresponding receptors, causing different biological consequences¹⁰. Among them, PI3K and PTEN are major regulators of AKT^{11,12}. Evidence indicates that AKT is often dysregulated in cancer¹³; however, the underlying mechanism is still not fully understood despite many years of investigations. In particular, it is not known whether lncRNAs are involved in the regulation of AKT activity.

Given the critical role of AKT in cell signalling, we design a screen system based on CRISPR/Cas9 synergistic activation mediator (SAM)¹⁴ and an AKT reporter to identify lncRNAs as AKT regulators. Through this screen, validation and further characterization we show that AK023948 positively regulates AKT activity by interaction with DHX9 and the regulatory subunit of PI3K.

Results

AK023948 as a positive AKT regulator. A variety of utilities of CRISPR/Cas9 system have been explored such as gene activation¹⁵ or repression¹⁶. Regarding gene activation, a recently reported SAM system uses MS2 bacteriophage coat proteins combined with p65 and HSF1, and it significantly enhances the transcription activation¹⁴. Therefore, we adopted this system for lncRNAs and designed gRNAs (five gRNAs for each lncRNA) covering ~1 kb upstream of the first exon to activate the endogenous lncRNAs. We focused on a specific group of lncRNAs (Supplementary Data set 1) primarily based on two sources (www.lncrnadb.org and <http://www.cuilab.cn/lncrnadisease>).

For screening, we designed an AKT reporter (Fig. 1a) because the AKT pathway is at the centre of cell signaling. This reporter system takes advantage of the Foxo transcription factors as direct targets of AKT and is capable of binding to forkhead response elements. Phosphorylation of Foxo by pAKT causes subcellular redistribution of Foxo, followed by rapid degradation¹⁷. Thus, the reporter vector carries three copies of forkhead response

element at the upstream of the well-known fusion repressor tetR-KRAB, which binds to the corresponding tet operator (tetO)^{18–20} in the same vector. The tetO controls the puromycin gene (Pu) and mCherry (tetO-Pu-T2A-mC). It is able to confer resistance to puromycin when no tetR-KRAB is bound on the tetO site. However, when tetR-KRAB binds to the tetO site, Pu is suppressed and the cells carrying this reporter become sensitive to puromycin. Since vector control or unrelated gRNAs (u-gRNAs) have no effect on pAKT and the level of Pu is low because of suppression by tetR-KRAB, few cells are expected to survive (Fig. 1a, top). However, if a certain gRNA can induce lncRNAs, which are capable of activating AKT (Fig. 1a, bottom), these cells are expected to survive and proliferate because little tetR-KRAB binds to the tetO site, and they are resistant to puromycin.

A screen procedure was outlined in Supplementary Fig. 1. After selection against puromycin, surviving cells were harvested. Compared with the cells before selection, after selection cells displayed an increase in pAKT at both T308 and S473 (Fig. 1b). Total RNA was extracted from the pooled after selection cells and before selection cells; lncRNA profiling by reverse transcriptase PCR (RT-PCR) arrays revealed that several candidate lncRNAs (Supplementary Fig. 2A) including AK023948 were upregulated presumably because of function of the corresponding SAM gRNAs. We chose AK023948 (the top of list) for further characterization. We confirmed that AK023948 gRNAs were able to increase the endogenous AK023948 (Supplementary Fig. 2B). In addition, AK023948 gRNAs conferred puromycin resistance for the cells carrying the AKT reporter (Supplementary Fig. 2C) and enhanced AKT activity (Fig. 1c).

AK023948-mediated AKT activation. AK023948 is a single exon gene with 2,807 bp (ref. 21). Further experiments with manipulation of AK023948 expression demonstrated that AK023948 promoted the AKT activity. For example, ectopic expression of AK023948 (Supplementary Fig. 3A) increased the pAKT level (Fig. 2a, left). In contrast, suppression of AK023948 by RNA interference (RNAi; Supplementary Fig. 3B) reduced the pAKT level (Fig. 2a, right; Supplementary Fig. 3C). To better determine the role of AK023948 in AKT activation, we generated AK023948 knockout (KO) by CRISPR/Cas9 using a dual gRNA approach²² (Supplementary Fig. 4). This AK023948 effect on AKT was more obvious in AK023948 KO clones (Fig. 2b). To further determine the role of AK023948 in activation of AKT, we re-expressed AK023948 in the KO cells, that is, rescue experiment. In both KO clones, re-expression of AK023948 was able to enhance the pAKT level (Fig. 2c; Supplementary Fig. 5A). In consistence with this finding, AK023948 KO also caused downregulation of the phosphorylation of PDK1 (Supplementary Fig. 5B), a known immediate upstream kinase of AKT, and re-expression of AK023948 was able to enhance PKD1 phosphorylation (Supplementary Fig. 5B). Although AK023948 is imbedded in thyroglobulin (TG) and Src-like-adaptor (SLA)²¹, we found little effect of AK023948 KO on SLA, as determined by qRT-PCR (Supplementary Fig. 5C), and TG was undetectable in these cells. In addition, we detected a positive correlation between AK023948 and pAKT in breast cancer tissue microarrays (TMA), where we first detected AK023948 by *in situ* hybridization (ISH; Fig. 2d) and then treated the previously ISH-stained TMAs by the acid/alcohol method^{23,24} to remove the AK023948 signal (Supplementary Fig. 6) before immunohistochemistry (IHC) staining for pAKT (Fig. 2d). For instance, 34 of 65 cases revealed low levels of both AK023948 and pAKT and 20 of 65 cases were high for both AK023948 and pAKT (Fig. 2e). Finally, IHC analysis of xenograft tumours derived from AK023948

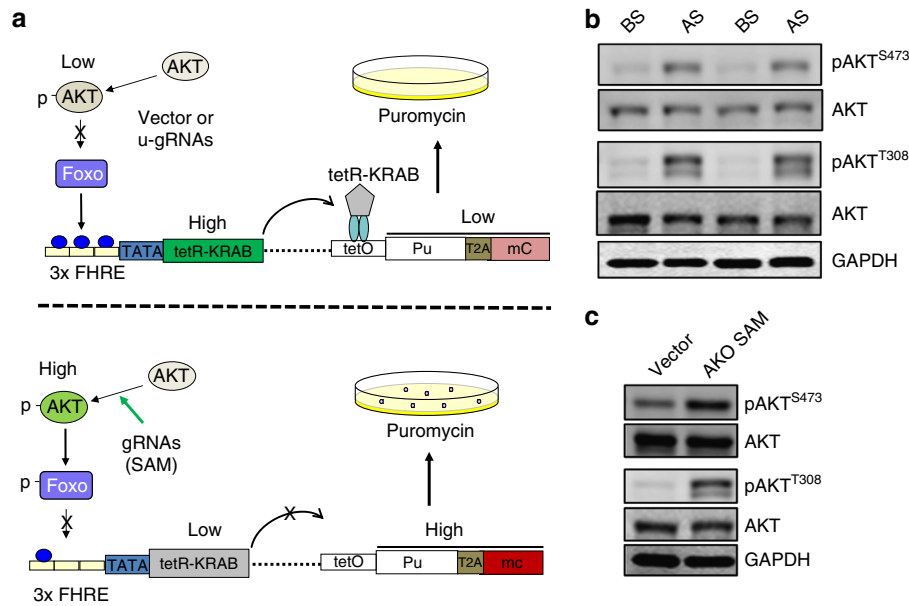


Figure 1 | Identification of lncRNAs capable of activating AKT by SAM library screen along with an AKT reporter. (a) Schematic description of principle for the AKT reporter used to screen the SAM library. SAM gRNAs that can activate AKT activity are enriched by puromycin selection. (b) Detection of AKT activity for cells before selection (BS) and cells after selection (AS) by western blot. (c) AKO23948 SAM gRNA increases the pAKT level. A mixed pool of five SAM gRNAs against AKO23948 were introduced into MCF-7 cells carrying dCas9-VP64 and pMS2-p65-HSF1 by infection and cellular extract was prepared for western blot 2 days after infection.

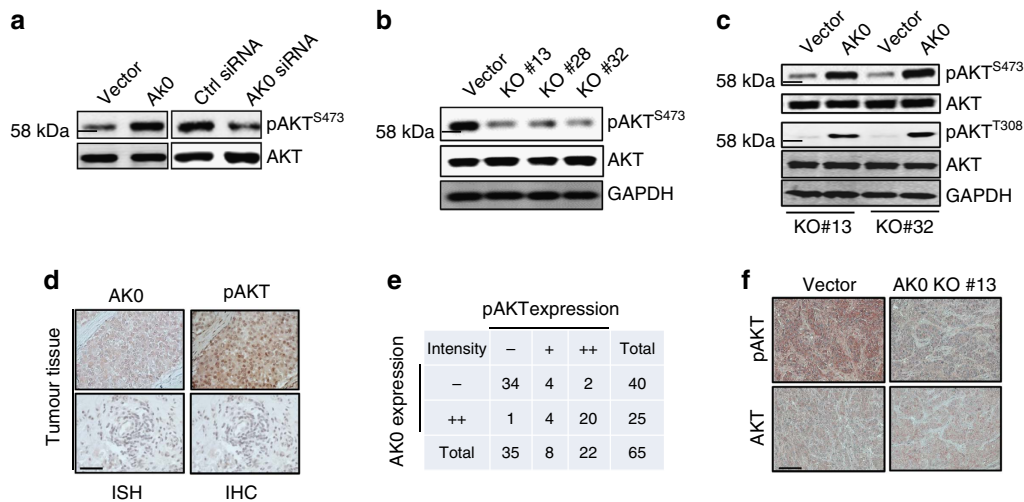


Figure 2 | AKO23948 regulates the pAKT level. (a) While AKO23948 overexpression increases, AKO23948 knockdown decreases phosphorylation of AKT. MCF-7 cells were transfected with either AKO23948 expression vector or AKO23948 siRNA. Cellular extract was prepared for western blot 48 h after transfection. (b) AKO23948 KO suppresses the pAKT level. AKO23948 KO was performed in MCF-7 using a procedure as described in Methods. (c) Re-expression of AKO23948 in the AKO23948 KO cells increases the pAKT level. AKO23948 expression vector or control vector was introduced into KO cells, and total cellular extract was prepared for western blot. (d) High levels of AKO23948 and pAKT in breast tumour specimens with representative images for the same field of a tumour. The same TMA was first detected for AKO23948 by ISH and then the signal was stripped, followed by IHC to detect pAKT. Scale bar, 100 μm. (e) A positive correlation between AKO23948 and pAKT from the same TMA with *P*-value of Fisher’s exact test for the association < 0.0001. (f) The pAKT level is lower in xenograft tumours derived from AKO23948 KO than in vector control tumours, as detected by IHC. Scale bar, 50 μm.

KO or vector control indicated that AKO23948 KO caused a remarkable reduction of the pAKT level (Fig. 2f).

Role of DHX9 in the AKO23948-mediated AKT activation.
To determine the underlying mechanism of AKO23948-

mediated AKT activation, we performed RNA precipitation using a biotin-labelled AKO23948 RNA probe. When the precipitate was subject to SDS-PAGE analysis, followed by silver staining, we detected a unique band of ~140 kDa to AKO23948, which was missing in precipitates from either BC200 or PCGEM1 as a control probe (Fig. 3a; Supplementary Fig. 7). Mass

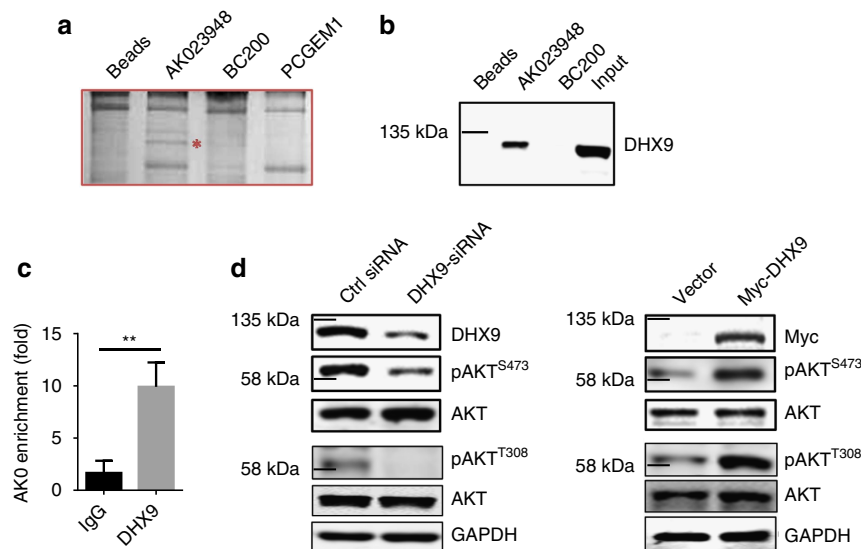


Figure 3 | DHX9 is an AKO23948-binding partner and is involved in regulation of AKT activity. (a) RNA precipitation using the biotin-labelled AKO23948 probe, followed by PAGE and silver staining. Red star indicates a unique band bound to AKO23948. Mass spectrometry analysis suggested DHX9 as a candidate. (b) Confirmation of the interaction between AKO23948 and DHX9 by RNA precipitation and western blot. (c) Confirmation of the interaction between AKO23948 and DHX9 by RNA immunoprecipitation using DHX9 antibody. (d) While DHX9 siRNA suppresses, ectopic expression of DHX9 increases the pAKT level. DHX9 siRNAs or DHX9 expression vector was introduced into MCF-7 cells by transfection, and cellular extract was prepared for western blot 48 h after transfection. Values in **c** are s.e.m. ($n = 3$). $**P < 0.01$ by two-tailed Student's *t*-test.

spectrometry analysis of this unique band was suggested as ATP-dependent RNA helicase A (RHA/DHX9). This result was confirmed by western blot analysis of the same RNA precipitate (Fig. 3b). To further confirm their interaction, we performed RNA immunoprecipitation (RIP) using DHX9 antibody and detected over a 10-fold enrichment of AKO23948 with DHX9 antibody over IgG control (Fig. 3c). To determine the role of DHX9 in AKT activation, we suppressed DHX9 by RNAi and ectopically expressed DHX9, respectively. We showed that DHX9 siRNAs reduced pAKT, whereas ectopic expression of DHX9 increased pAKT (Fig. 3d), suggesting that DHX9 is involved in the AKT pathway and interaction of DHX9 with AKO23948 may be required for the AKO23948-mediated AKT activation.

AKO23948 is required for the interaction of DHX9 with p85. DHX9 is a RNA helicase carrying various domains such as RBD1, RBD2, RGGG and helicase²⁵. In addition, DHX9 interacts with double-stranded nucleic acids and protein factors like NF- κ B p65 (ref. 26) and BRCA1 (ref. 27). In particular, DHX9 might also bind to the regulatory subunit of PI3K, p85, as suggested by mass spectrometry analysis²⁸. It is well known that PI3K consists of a regulatory subunit p85 and a catalytic subunit p110, and together they regulate AKT activity²⁹. With regard to the regulatory subunit, there are two major isoforms of p85, that is, p85 α and p85 β (ref. 13), and thus, we determined their relative expression levels. As shown in Supplementary Fig. 8A, we detected a fair amount of p85 β with p85 β antibody, but detected little p85 α with p85 α antibody in MCF-7 cells. Of interest, AKO23948 KO suppressed the p85 β level, but had little effect on p85 α (Fig. 4a; Supplementary Fig. 9A), suggesting that p85 β is a major target of AKO23948. Western blot using pan-p85 antibody also only detected p85 β isoform in 293T and MCF-7 cells (Supplementary Fig. 8B). Therefore, we performed RIP assays using the same pan-p85 antibody in the following experiments. As expected, AKO23948 interacted with p85,

revealing over a 3-fold enrichment as compared with IgG control (Fig. 4b). In addition, RNA precipitation with AKO23948 as a probe also detected p85 AKO23948, and both DHX9 and p85 can bind to the 3' region of AKO23948 (Supplementary Fig. 9B).

Co-immunoprecipitation assays confirmed the interaction of DHX9 with p85 in MCF-7 cells (Fig. 4c, top). Importantly, AKO23948 is required for this interaction. For example, HMLE cells express little AKO23948 (see Fig. 6b); no visible interaction between DHX9 and p85 was detected (Fig. 4c, bottom). Furthermore, AKO23948 KO abolished this interaction in MCF-7 cells (Fig. 4d, vector lane). Re-expression of AKO23948 in the AKO23948 KO cells was able to restore the ability of p85 to interact with DHX9 (Fig. 4d, last lane on the right). Glutathione S-transferase (GST) pulldown assays further indicated that AKO23948 is required for the interaction between DHX9 and p85 because the amount of DHX9 pulled down by GST-p85 was lower in AKO23948 KO than in gRNA control (Fig. 4e). Moreover, proximity ligation assay (PLA) revealed that suppression of AKO23948 by RNAi reduced the interaction between DHX9 and p85 (Fig. 4f; Supplementary Fig. 9C). Finally, DHX9 siRNAs suppressed both p85 and pAKT, whereas ectopic expression of DHX9 enhanced the p85 and pAKT level (Fig. 4g).

AKO23948 promotes the p85 stability. We further showed that AKO23948 and DHX9 regulated the stability of p85. For example, the half-life of p85 was ~ 5.5 h for vector control, whereas it was ~ 3.5 h in AKO23948 KO cells (Fig. 5a). Similarly, DHX9 siRNAs also decreased the p85 stability (Supplementary Fig. 10A) and p85 short interfering RNA (siRNA) reduced AKT activity (Supplementary Fig. 10B). However, DHX9 had no effect on AKO2398 expression (Supplementary Fig. 11A) or its subcellular distribution (Supplementary Fig. 11B). Together, these results suggest that both AKO23948 and DHX9 are involved in the regulation of the p85 stability.

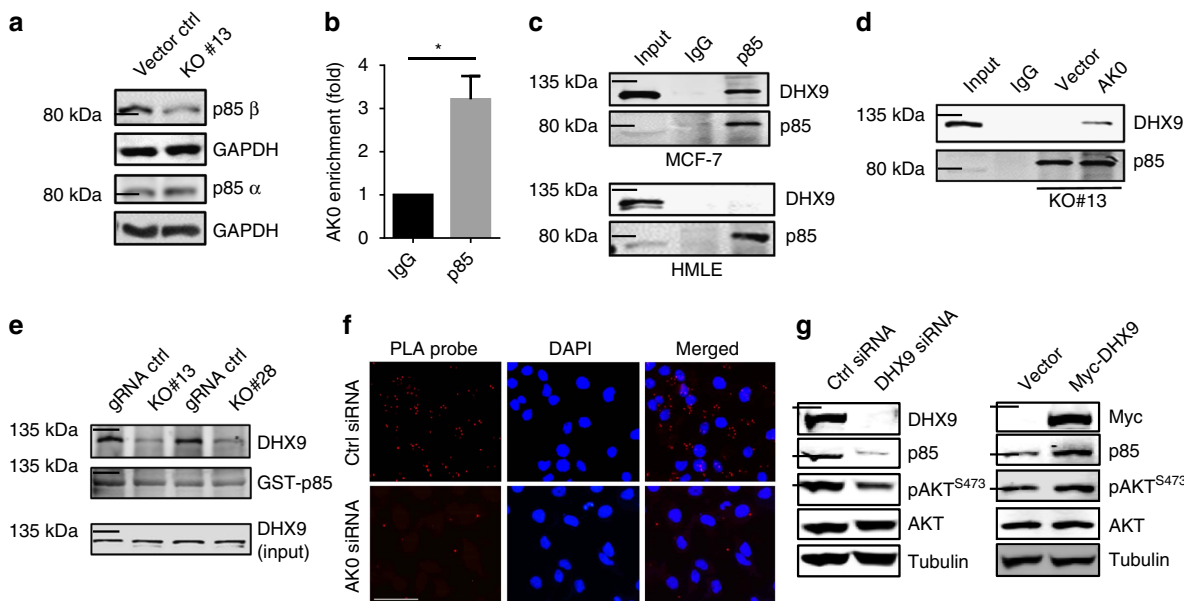


Figure 4 | AKO23948 is required for the interaction between DHX9 and p85. (a) AKO23948 KO primarily suppresses the p85 β level, as detected by western blot. (b) AKO23948 interacts with p85, as detected by RIP assay using p85 antibody. (c) AKO23948 is required for the interaction between DHX9 and p85, as detected by co-immunoprecipitation (co-IP) using p85 antibody. HMLE cells express little AKO23948, whereas MCF-7 cells express a high level of AKO23948. (d) Rescue experiments further suggest that AKO23948 is critical for the interaction between AKO23948 and p85. (e) AKO23948 is required for the interaction between DHX9 and p85, as determined by GST pull-down assay. The DHX9 level pulled down by GST-p85 was lower in KO cells than in gRNA control. (f) AKO23948 is required for the interaction between DHX9 and p85, as detected by the Duolink *in situ* Fluorescence Kit (Sigma). HeLa cells were transfected with Myc-p85 plus control siRNA or AKO siRNA. After 48 h, the cells were fixed for PLA. The red signals were lower in AKO siRNA than in control siRNA cells. Scale bar, 100 μ m. (g) DHX9 siRNAs suppress, but ectopic expression of DHX9 increases both p85 and pAKT. Values in **b** are s.e.m. ($n = 3$). * $P < 0.05$ by two-tailed Student's *t*-test.

Next, we showed that AKO23948 affected the interaction between p85 and p110 because AKO23948 KO reduced their interaction (Fig. 5b). Receptor tyrosine kinases (RTKs) are major kinases responsible for activation of PI3K, which then converts phosphatidylinositol-3,4-diphosphate to phosphatidylinositol (3,4,5)-trisphosphate to serve as a secondary messenger. To determine the role of AKO23948 in RTK-mediated AKT activation, we first cultured the cells in serum-free medium for 2 h and then treated the cells with epidermal growth factor (EGF) or insulin at 10 ng ml⁻¹. As expected, no pAKT was detected during serum starvation, and EGF or insulin induced AKT activity (Fig. 5c). However, this EGF/insulin-induced AKT activation was severely inhibited in AKO23948 KO cells (Fig. 5c). In addition, we starved the cells for 12 h and then added insulin for 5~90 min. Again, the insulin-induced AKT activity was substantially decreased in AKO23948 KO cells as compared with gRNA control (Supplementary Fig. 12A,B). Similarly, acidosis-induced AKT activity³⁰ was also impaired in AKO23948 KO cells (Fig. 5d; Supplementary Fig. 12C).

ERK is a downstream target of RAS and RTKs. After activation, RTKs can also recruit RAS which subsequently interacts with the catalytic subunit of PI3K, p110, to activate AKT³¹⁻³³. Of interest, AKO23948 KO had little effect on the pERK level whether EGF/insulin is absent or present (Fig. 5e; Supplementary Fig. 12A,B), providing additional evidence that AKO23948 acts on p85, but not p110, to activate AKT. PTEN is a well-known tumour suppressor³⁴. As a phosphatase, PTEN reverses PI3P to PI2P and thus functions as a suppressor for AKT. BT549 is a PTEN-deficient cell line such that the pAKT level is high as compared with that in MCF-7 cells (Fig. 5f). However, AKO23948 siRNA was still able to suppress the pAKT level (Fig. 5f;

Supplementary Fig. 12D). Finally, AKT inhibitors such as PP2A³⁵ can act on AKT; suppression of PP2A by okadaic acid increased pAKT levels³⁶; however, the induction was lower in KO cells than in control cells (Supplementary Fig. 12E).

Clinical significance of AKO23948 and DHX9. In consistence with upregulation of AKT activity by AKO23948, we showed that AKO23948 was highly expressed in breast tumour tissue compared with normal breast tissue (Fig. 6a). Moreover, the AKO23948 level was also higher in cancer cell lines MCF-7 and MDA-MB-231 cells than in non-malignant cells HMLE and MCF-10A (Fig. 6b). These results suggest that AKO23948 may play an oncogenic role. Indeed, MTT assays indicated that AKO23948 siRNA significantly suppressed cell growth *in vitro* (Supplementary Fig. 13A). In contrast, ectopic expression of AKO23948 promoted cell growth (Supplementary Fig. 13B). Furthermore, cell growth for AKO23948 KO cells was significantly reduced compared with gRNA control (Fig. 6c; Supplementary Fig. 13C) and AKO23948 KO caused more apoptosis (Fig. 6d; Supplementary Fig. 14). Experiments with xenograft mouse model revealed that AKO23948 KO remarkably inhibited tumour growth rate (Fig. 6e) and tumour weight (Supplementary Fig. 15A). In consistence with this result, IHC analysis of xenograft tumours revealed that AKO23948 KO caused a substantial decrease in the level of the proliferation marker Ki-67 (Supplementary Fig. 15B). ISH of breast TMA provided further evidence that AKO23948 was upregulated in breast tumours as compared to normal tissue (Fig. 6f). For example, 71% of breast tumour specimens was positive for AKO23948, whereas only 9.5% of normal breast tissue was positive for AKO23948.

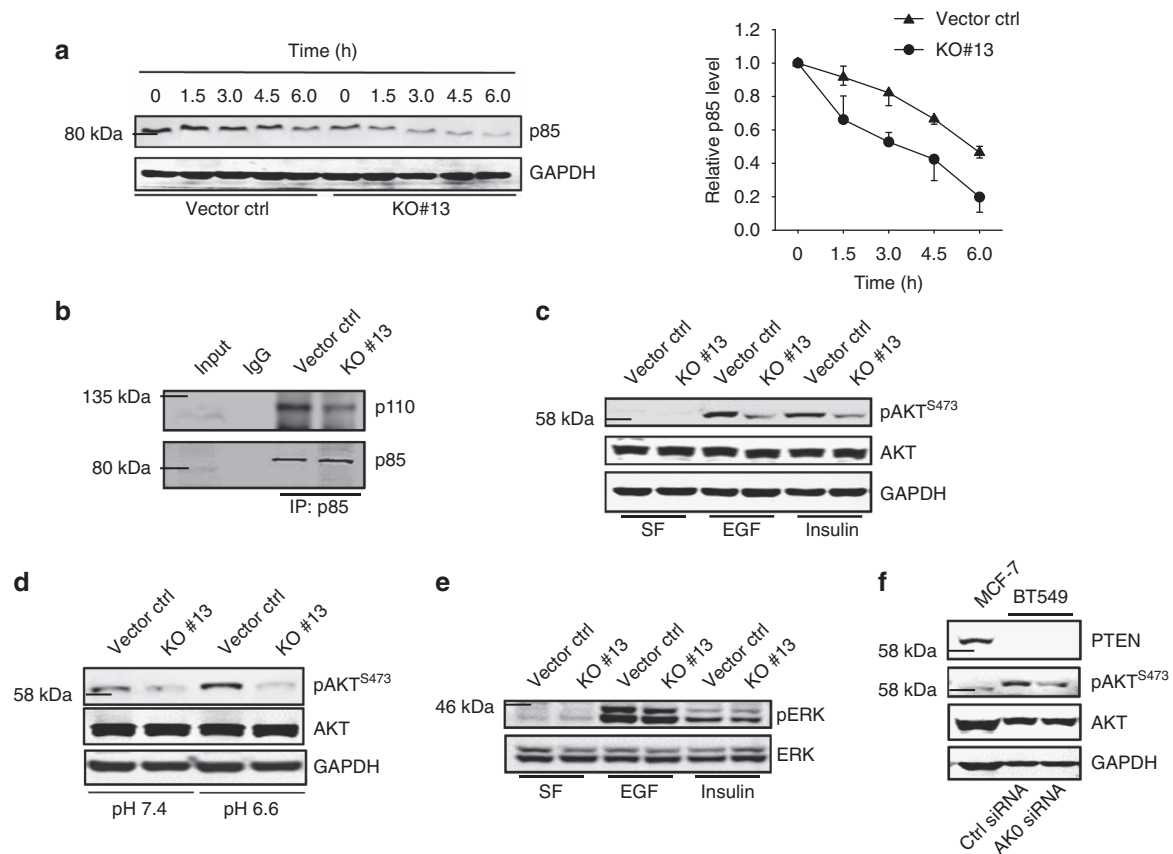


Figure 5 | AKO23948 has an impact on the p85 stability. (a) Effect of AKO23948 KO on the p85 stability. MCF-7 cells were treated with cycloheximide (CHX) at $20 \mu\text{g ml}^{-1}$ and then were harvested for western blot at indicated time points. Half-life curve is on the right. (b) AKO23948 KO reduces the interaction of p85 with p110, as detected by co-IP. (c) AKO23948 KO inhibits the growth factor-induced AKT activation. Cells were first cultured in a serum-free medium for 2 h and then EGF or insulin was added at 10 ng ml^{-1} for 30 min. (d) AKO23948 KO inhibits the acidosis-induced AKT activation. Cells were cultured at pH 7.4 or pH 6.6 for 2 h before harvesting for western blot. (e) AKO23948 KO has no effect on ERK activity. Cells were treated with the same way as in c. (f) Suppression of AKO23948 by RNAi can still reduce the pAKT level in PTEN-deficient BT549 cells.

Given the role of DHX9 in AKT activity, we interrogated the Cancer Genome Atlas-invasive breast carcinoma data set at cBioportal (<http://www.cbioportal.org/>)^{37,38} and found that DHX9 was upregulated in 21% of 1,091 cases (Supplementary Fig. 16A, top). Importantly, this upregulation of DHX9 was positively associated with poor overall survival (Fig. 6g). For example, median months survival for cases with DHX9 upregulation were 83.25, whereas the median months survival for cases without DHX9 upregulation were 114.73 (Supplementary Fig. 16A, bottom). Furthermore, DHX9 was also upregulated in breast cancer cell lines as compared with non-malignant HMLE cells (Supplementary Fig. 16B). Together, these results highlight the clinical significance of AKO23948 and DHX9.

Discussion

Activation of the AKT pathway in cancer has been extensively investigated in past decades¹³, which has demonstrated a critical role of PI3K in tumorigenesis by regulation of AKT activity. While it is well known now that oncogenic mutations in PI3K genes can contribute to upregulation of AKT activity in cancer, little is known how PI3K itself is regulated. In the present study, we provide evidence that AKO23948 is required for AKT activation through interaction with DHX9 and p85. Our study suggests that the interaction of AKO23948 with

p85 and DHX9 is critical for AKT activation in response to growth factors and environmental stress such as acidosis. Therefore, AKO23948 and DHX9 are previously uncharacterized important players in the AKT pathway.

DHX9 is a DEAD box protein with RNA helicase activity²⁵. It may participate in melting of DNA:RNA hybrids, such as those that occur during transcription. Of interest, DHX9 can interact with many proteins including BRCA1 (ref. 27), KHDRBS1 (ref. 39), AKAP8L (ref. 40) and NXF1 (ref. 41). Thus, DHX9 is implicated in a number of cellular processes involving alterations of RNA secondary structure such as translation initiation, nuclear and mitochondrial splicing, and ribosome and spliceosome assembly. However, up to date there is no evidence that DHX9 is involved in AKT activity. Our study demonstrates that as an AKO23948-binding partner, DHX9 along with AKO23948, regulates the p85 stability. For example, AKO23948 KO or suppression of DHX9 by RNAi significantly decreases the half-life of p85.

Activation of AKT is a complicated process, which involves vast arrays of players, starting at RTK. Upon activation of RTK by growth factors, PI3K is capable of generating the second messenger phosphatidylinositol (3,4,5)-trisphosphate, which subsequently activates critical downstream targets such as AKT and mammalian target of rapamycin. When dysregulated, the PI3K pathway has a causal role in many forms of cancer,

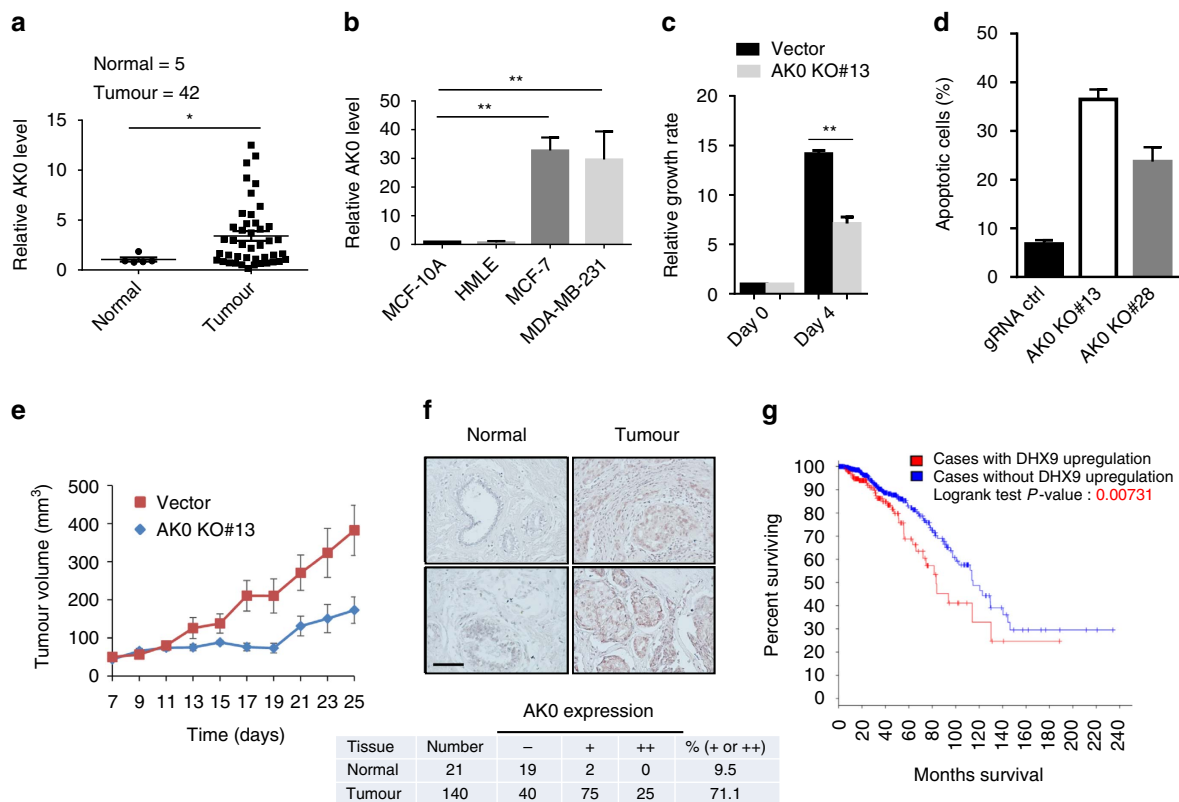


Figure 6 | Upregulation of AKO23948 in breast cancer and promotion of tumorigenesis. (a) Detection of AKO23948 in the OriGene breast cancer tissue cDNA array by qPCR. (b) AKO23948 is upregulated in breast cancer cells (MCF-7 and MDA-MB-231) as compared with non-malignant breast cells (MCF-10A and HMLE). (c) AKO23948 KO suppresses cell proliferation of MCF-7, as detected by MTT assay. (d) AKO23948 KO promotes apoptosis. Cells were seeded in slide chambers, and treated with H₂O₂ at 0.8 mM for 4 h before TUNEL assay. Apoptotic cells were counted from three different fields, and apoptotic cell ratio was calculated against total cells. (e) Tumour growth for vector control and AKO KO#13 in nude mice. (f) Expression of AKO23948 in breast cancer TMAs, as detected by ISH. Scale bar, 100 μ m. Bottom: quantitative analysis of AKO23948 expression based on the results from f. (g) Upregulation of DHX9 expression is associated with poor patient survival. About 20.9% (229 of 1091 cases analysed) are positive for DHX9 using the Onco Query Language (OQL; EXP>1.5). Values in b,c are s.e.m. (*n* = 3). ***P* < 0.01 by two-tailed Student's *t*-test.

including breast cancer⁴². Despite the importance of p85 in the AKT pathway, information about the regulation of p85 is limited. Nevertheless, a recent report suggests that the short isoform of ErbB3-binding protein 1, p42, is able to increase degradation of p85, leading to a decreased AKT activity and tumorigenesis⁴³. Our study suggests an additional mechanism by which AKO23948 and DHX9 can regulate the stability of p85. Given that DHX9 interacts with AKO23948, it is conceivable that activation of the PI3K complex requires both AKO23948 and DHX9.

The PI3K regulatory subunit consists of two major isoforms, that is, p85 α and p85 β , but evidence indicates that they have an opposite effect on AKT activity and tumorigenesis. For instance, KO experiments suggest that p85 α functions as a tumour suppressor⁴⁴, which is also supported by the findings that p85 α is downregulated in cancer specimens^{45,46}. Moreover, p85 α deletion increases tumorigenesis. A functional missense mutation in p85 α resulting in reduced p85 expression is associated with colon cancer⁴⁷. In contrast to p85 α , p85 β plays an oncogenic role. Upregulation of p85 β is found in several cancers, and in an experimental setting p85 β drives tumour progression⁴⁶. Expression of p85 β induces oncogenic transformation of primary avian fibroblasts⁴⁸. In support of these findings, we show that p85 β is a primary target for AKO23948 in breast cancer cells.

Although lncRNAs are poorly characterized in general, emerging evidence indicates that lncRNAs may function as

oncogenes and tumour suppressors, thus having an impact on one or more of the cancer hallmarks⁴⁹. While much has been learned in the past years about the role of a small number of lncRNAs in cancer such as HOTAIR, little is known about AKO23948. In this regard, our study suggests an oncogenic role of AKO23948 in breast cancer, in contrast to what has been reported in papillary thyroid cancer²¹. This is based on these lines of evidence. (1) AKO23948 is upregulated in breast cancer and its expression is correlated with pAKT in clinical specimens. (2) While ectopic expression of AKO23948 promotes, AKO23948 siRNA or AKO23948 KO suppresses AKT activity, and tumour cell growth. (3) Re-expression of AKO23948 in AKO23948 KO cells is able to restore the AKT activation. (4) As an AKO23948-binding partner, DHX9 is also upregulated in breast tumours; this upregulation is associated with poor overall survival. Importantly, our results further suggest that this AKO23948-mediated AKT activation is at least in part through interaction with DHX9 and p85. Hence, these results provide a molecular basis that AKO23948 plays an oncogenic role in breast cancer.

In summary, our screen system provides a platform for identification of AKT-associated lncRNAs. Furthermore, our study suggests that AKO23948 functions as a positive regulator for AKT (Supplementary Fig. 17). AKO23948 is required for the interaction DHX9 and p85, as suggested co-immunoprecipitation and GST pulldown assays, and is also critical to AKT activity in

response to various stimuli such as growth factors or acidosis. In normal cells, the AK023948 level is low, and thus, the AKT activity is low even in the presence of growth factors. This low AKT activity may also be attributed to the low level of DHX9. In the tumour cells, upregulation of AK023948 and DHX9 leads to a high activity of AKT. Several reports indicate that upregulation or mutation in p85 and p110 may contribute to an elevated level of pAKT and cancer development^{50,51}. Our results suggest an additional mechanism for regulation of AKT activity. Thus, these tumour cells become more proliferative and aggressive.

Methods

Reagents. Primary antibodies were purchased from the following sources: pAKT^{T473} (#4060), pAKT^{S308} (#2965), AKT (#2920), p85 (#4257), p110 (#4249), pERK (#4370), ERK (#4696) from Cell Signaling (Danvers, MA); DHX9 (#26271), p85 α (#191606) and p85 β (#180917) from Abcam (Cambridge, MA). Most of western blots were performed at 1,000 \times dilution of primary antibodies. GAPDH and tubulin from ProteinTech (Chicago, IL), PTEN (#7974) was from Santa Cruz (Dallas, TX). Secondary antibodies conjugated with IRDye 800 CW or IRDye 680 were purchased from LI-COR Biosciences (Lincoln, NE). PCR primers were obtained from IDT (Coralville, IA). AK023948 siRNAs and control siRNA were purchased from Fisher Scientific (Pittsburgh, PA). DHX9 siRNAs (#sc-45706, pooled) and p85 β siRNAs (#sc-39125, pooled) were purchased from Santa Cruz. Transfection of siRNAs was carried out at 50–100 nM concentration. AK023948 LNA probe and control oligos for ISH was purchased from Exiqon (2950 Vedbaek, Denmark). Breast cancer TMAs were purchased from US Biomax (Rockville, MD). Commercial cDNA arrays of breast cancer tissues were purchased from OriGene (Rockville, MD).

Cell culture. Breast cancer cell lines MCF-7 and MDA-MB-231 (ATCC, Manassas, VA) were grown in RPMI 1640 (Fisher Scientific) with 10% FBS (Sigma-Aldrich) and 2 mM glutamine. MCF-10 A (ATCC) and HMLE cells (Dr Robert A. Weinberg, The Massachusetts Institute of Technology) were grown in DME/F-12 (Fisher Scientific) with 5% FBS, 2 mM glutamine, along with 20 ng ml⁻¹ EGF, 10 μ g ml⁻¹ insulin and 0.5 μ g ml⁻¹ hydrocortisone. All the media were supplemented with 100 units of penicillin per ml and 100 μ g of streptomycin per ml (Fisher Scientific). MCF-7 cells were used in SAM library screen. MCF-7 and MDA-MB-231 cells were authenticated by DDC Medical (<http://www.ddcmedical.com>) using the short tandem repeat profiling method. Mycoplasma test was performed by PCR amplification method (Applied Biological Materials, Richmond, BC, Canada).

MTT assay. MTT assay was performed to determine the effect of AK023948 on cell growth. Approximately 2,000 cells were seeded in triplicate into 96-well plates and grown for 3 days before MTT assay.

Transfection. Cells were transfected with plasmid DNA using DNAfectin (Applied Biological Materials) or with siRNAs using RNAfectin reagent (Applied Biological Materials) following the manufacturer's protocol.

Lentivirus infection. Lentivirus was packaged in 293T cells using pPACK packaging mixture (SBI) and the virus containing culture medium was collected and spun for 10 min at 3,000 r.p.m. for 48 h after transfection. Lentivirus infection was carried out six-well plates by mixing 500 μ l virus supernatant + 500 μ l medium containing 8 μ g polybrene at multiplicity of infection < 1.

Western blot. The cells were treated as per requirement, and total protein was harvested from cells using lysis buffer (20 mM Tris, pH 8.0; 100 mM NaCl; 1 mM EDTA; 0.5% NP-40; 10% glycerol). Concentration of protein was estimated by Bradford method⁵². The protein samples were run in SDS-PAGE and probed with an antibody of interest.

Verification of AK023948 transcript. We performed 5' RACE using a previous described procedure⁵³, followed by PCR with primers AKO-polyT adaptor, AK0-adaptor and AK0-5Race-3.2 (Supplementary Data set 2). For 3' RACE we first added poly adenosine by poly A polymerase (NEB) and then reverse transcribed using AKO-polyT adaptor primer. PCR used primers AK0-3Race-5.1 and AKO-adaptor-5.1 (Supplementary Data set 2). The resulting PCR product was cloned into pCR8 for DNA sequencing.

GST pulldown assay. PIK3R2 (p85 β) was cloned into pGEX-2T at EcoRI and BamHI, and GST-p85 β fusion protein was purified by Glutathione Sepharose 4B (GE Healthcare Life Sciences) according to the manufacturer's protocol.

Cellular extracts from gRNA control or AK0 KO#13 and KO#28 were used for pulldown assays.

Generation of SAM library. Five gRNAs were designed for each lncRNAs as in shown in Supplementary Data set 1. In addition, 10 gRNAs against non-human genes were designed as negative controls with a total 1,215 gRNAs in this pool. The lncRNA-specific gRNAs were designed using Chop-Chop programme⁵⁴ against ~1 kb upstream of the first exon of lncRNAs. Oligonucleotides carrying each gRNA were synthesized as a mixed pool (CustomArray Inc.) and then amplified by PCR using primers SAM gRNA-5.1 and SAM gRNA-3.1 and finally cloned into a modified pMS2 vector by Gibson assembly method⁵⁵.

Screen procedure. We subsequently introduced dCas9-VP64 and pMS2-p65-HSF1 (ref. 14) into MCF-7 cells by infection and established stable transductants. Next, we introduced SAM library or vector control by infection. Finally, we introduced the AKT reporter. Potential clones were selected in the presence of puromycin at 0.5 μ g ml⁻¹ for 5 days. To determine which gRNAs are enriched, we pooled surviving cells and isolated total RNAs, and then profiled lncRNAs by qRT-PCR using primers against the targeted lncRNAs.

LncRNA profiling. LncRNA profiling (RT-PCR arrays) was performed in 96-well plates using SYBR Green method. Total RNA was isolated using Direct-zol RNA MiniPrep Kit (Zymo Research, Irvine, CA) as suggested by manufacturer. Reverse transcription was carried out by using RevertAid Reverse Transcriptase (Fisher Scientific) and random primer mix (New England BioLabs, Ipswich, MA). Analysis of qRT-PCR was performed as described previously⁵⁶. Delta-delta Ct values were used to determine their relative expression as fold changes.

Plasmid construction. Individual AK023948 SAM gRNAs were constructed by first annealing each pair of oligos (Supplementary Data set 2) and ligating them to BsmBI-linearized pMS2 vector¹⁴. AK023948 expressing vector was generated in pCDH-MSCV-EF1-GFP-T2A-Pu (System Biosciences) using PCR primers AK023948-R1-5.1 and AK023948-Not1-3.1. The same approach was used to clone DHX9 with N-terminal Myc tag. Dual gRNA cloning for AK023948 KO was performed as previously described²². In brief, AK023948 donor vector was constructed using primers AK023948-right-R1-5.1 and AK023948-right-R1-3.1; AK023948-left-BamHI-5.1 and AK023948-left-BamHI-3.1. GST-p85 was constructed by PCR using primers pGEX-2T-BamHI-PI3KR2-5.1 and pGEX-2T-R1-PI3KR2-3.1, and then cloned into pGEX-2T at BamHI and EcoRI sites. Myc-p85 was constructed by PCR using primers PI3KR2-R1-Myc-5.1 and PI3KR2-Not1-3.1 and then cloned into pCDH-CMV-EF1-Pu (System Biosciences) at EcoRI and NotI sites. The high-fidelity DNA polymerase Phusion enzyme (New England BioLabs) was used for PCR. All PCR products were verified by DNA sequencing.

AK023948 KO by CRISPR/Cas9. Selection of AK023948 KO clones in MCF-7 cells was carried out using the procedure as described previously²². Briefly, AK023948 dual gRNA and donor vector were co-transfected into the MCF-7 cells in six-well plate using DNAfectin (Applied Biological Materials). Next day the cells were re-seeded in 10 cm dishes. After 6 days of transfection, puromycin was added 0.5 μ g ml⁻¹ to cell culture and were further grown for 14 days. Individual puromycin resistant colonies were picked up manually and then expanded in 12-well plates. Initial identification of KO clones was carried out by genomic PCR. Positive clones were further verified by qRT-PCR.

RNA precipitation. To identify the AK023948-binding partner, we prepared AK023948-biotinylated RNA probe that was used to pulldown assays for whole-cell lysate. To prepare the probe we first introduced T7 promoter in front of the AK023948 by using PCR primers AK023948-T7-5.1 and AK023948-Not1-3.1 (Supplementary Data set 2). The amplified sequence was then cloned into pCR8 vector (Fisher Scientific). The resultant plasmid was then linearized with NotI and used for *in vitro* RNA synthesis. Total cellular extract was used to mix well with the RNA probe, followed by precipitation using streptavidin agarose beads (Fisher Scientific). BC200 and PCGEM1 served as negative controls in addition to beads alone. The protein attached to beads was separated in PAGE. Silver staining was carried out using Pierce Silver Staining Kit (Fisher Scientific) following their protocol. The band unique to AK023948 was cut out and sent for mass spectrometry analysis (Applied Biomics, Hayward, CA).

RNA immunoprecipitation. RNA immunoprecipitation was performed using the Magna RIP RNA-Binding Protein Immunoprecipitation Kit (Millipore, Billerica, MA) and different antibodies (p85 and DHX9) according to the manufacturer's protocol. After the RNA was recovered from protein A + G beads, qRT-PCR was performed to detect AK023948.

In situ hybridization. Biotinylated AK0-LNA probe (Supplementary Materials) was used for ISH as previously described⁴. In brief, following pre- and hybridization, and washes, the signal was amplified by TSA amplification kit (Perkin Elmer) and subsequently revealed by Ultra Vision One polymer and AEC chromogen (Fisher Scientific). The intensity of signal in TMA was classified as – (negative), + (weak positive) and ++ (strong positive). To make sure that ISH is specific to AK023948, we designed a blocker which is a complementary sequence of AK0-LNA probe. We used 10 times higher concentration of blocker than AK0-LNA during hybridization. Procedure for fluorescence *in situ* hybridization was essentially same as above except that signals were revealed by TSA Kit #24 with Alexa Fluor 568 (Life Technology).

Immunohistochemistry. To detect pAKT in clinical samples we re-used the TMA, which was previously used to detect AK023948 by ISH. We treated the TMA in 1% acid alcohol (HCl + ethanol) for 1 min to remove the horseradish peroxidase (HRP) signal from ISH^{23,24}. After washing, the slide was boiled in 10 mM sodium citrate at pH 6 and treated with 3% H₂O₂, and then blocked in 3% BSA. Finally, the slide was probed with pAKT antibody, using ultravision one detection system HRP polymer and AEC chromogen (Fisher Scientific) following the manufacturer's protocol. The clinical correlation between pAKT and AK023948 expression was determined by Fisher's exact test for association.

Co-immunoprecipitation. Corresponding antibody or IgG was added to cell lysate that was treated with A + G agarose beads (Fisher Scientific). The mixture was rotated for 1.5 h and precipitated beads were washed three times with PBS containing protease inhibitor cocktail. The protein lysates were separated in SDS-PAGE.

Proximity ligation assay. PLA was carried out using Duolink *in situ* fluorescence kit (#DUO92101 from Sigma) according to the manufacturer's protocol. In brief, HeLa cells were simultaneously transfected with Myc-p85 plus control siRNA or AK0 siRNA in culture chambers and 48 h later, the cells were fixed with 4% paraformaldehyde and permeabilized with 0.1% Triton X, followed by 3% BSA for blockage. Myc tag (mouse) and DHX9 (Rabbit) antibody were added and incubated at 4 °C overnight. Secondary antibodies conjugated with oligonucleotides (Rabbit antibody with PLA probe plus and Mouse antibody with PLA probe minus) were incubated for 1 h at 37 °C after primary antibody. After wash, ligation was taken place for 30 min at 37 °C, followed by amplification with polymerase for 2 h at 37 °C.

Animal work. Female nude (nu/nu) mice (4~5 weeks old) were obtained from Harlan Laboratories (Indianapolis, IN). All animal studies were conducted in accordance with the NIH animal use guidelines and a protocol was approved by the School's Animal Care Committee. MCF-7 AK023948 KO#13 and MCF-7 gRNA vector control cells were harvested at exponential growth stage and mixed with 50% matrigel (BD Biosciences, Franklin Lakes, NJ). One million cells/spot were injected to mammary fat pad of mouse as described earlier⁵⁷. Growth of tumours was monitored and measured every other day after 7 day of tumour cell injection. The volume of tumour was calculated by using formula, $V = 1/2 (\text{width}^2 \times \text{length})$.

Statistical analysis. Although the researchers conducting the experiments were not blinded to the group allocation, statistician was blinded from group allocation when performing statistical analyses. The continuous outcomes were summarized as the mean and s.e.m. The normality of data was checked by the stem and leaf plot, and the data were approximately normal. The two-sample *t*-test was used to compare the mean of continuous outcome between two experimental conditions. The Satterthwaite *t*-test was used when unequal variances were confirmed by Levene's test. The Bonferroni correction was applied in the experiments involving comparisons at multiple time points or among more than two experimental conditions. The Kaplan–Meier method was used to estimate the survival probability in subgroups determined by expression level of DHX9.

Data availability. The authors declare that all the data supporting the findings of this study are available within the article and its Supplementary Information files and from the corresponding author upon reasonable request.

References

- Consortium, E. P. *et al.* Identification and analysis of functional elements in 1% of the human genome by the ENCODE pilot project. *Nature* **447**, 799–816 (2007).
- Tsai, M. C. *et al.* Long noncoding RNA as modular scaffold of histone modification complexes. *Science* **329**, 689–693 (2010).
- Kino, T. *et al.* gas5 is a growth arrest- and starvation-associated repressor of the glucocorticoid receptor. *Sci. Signal.* **3**, ra8 (2010).
- Zhang, Z. *et al.* Negative regulation of lncRNA GAS5 by miR-21. *Cell Death Differ.* **20**, 1558–1568 (2013).
- Mercer, T. R., Dinger, M. E. & Mattick, J. S. Long non-coding RNAs: insights into functions. *Nat. Rev. Genet.* **10**, 155–159 (2009).
- Wang, K. C. & Chang, H. Y. Molecular mechanisms of long noncoding RNAs. *Mol. Cell* **43**, 904–914 (2011).
- Ulitsky, I. & Bartel, D. P. lincRNAs: genomics, evolution, and mechanisms. *Cell* **154**, 26–46 (2013).
- Hu, W., Alvarez-Dominguez, J. R. & Lodish, H. F. Regulation of mammalian cell differentiation by long non-coding RNAs. *EMBO Rep.* **13**, 971–983 (2012).
- Fresno Vara, J. A. *et al.* PI3K/Akt signalling pathway and cancer. *Cancer Treat. Rev.* **30**, 193–204 (2004).
- Los, M., Maddika, S., Erb, B. & Schulze-Osthoff, K. Switching Akt: from survival signaling to deadly response. *Bioessays* **31**, 492–495 (2009).
- Vanhaesebroeck, B., Stephens, L. & Hawkins, P. PI3K signalling: the path to discovery and understanding. *Nat. Rev. Mol. Cell Biol.* **13**, 195–203 (2012).
- Hollander, M. C., Blumenthal, G. M. & Dennis, P. A. PTEN loss in the continuum of common cancers, rare syndromes and mouse models. *Nat. Rev. Cancer* **11**, 289–301 (2011).
- Thorpe, L. M., Yuzugullu, H. & Zhao, J. J. PI3K in cancer: divergent roles of isoforms, modes of activation and therapeutic targeting. *Nat. Rev. Cancer* **15**, 7–24 (2015).
- Konermann, S. *et al.* Genome-scale transcriptional activation by an engineered CRISPR-Cas9 complex. *Nature* **517**, 583–588 (2015).
- Maeder, M. L. *et al.* CRISPR RNA-guided activation of endogenous human genes. *Nat. Methods* **10**, 977–979 (2013).
- Qi, L. S. *et al.* Repurposing CRISPR as an RNA-guided platform for sequence-specific control of gene expression. *Cell* **152**, 1173–1183 (2013).
- Brunet, A. *et al.* Akt promotes cell survival by phosphorylating and inhibiting a Forkhead transcription factor. *Cell* **96**, 857–868 (1999).
- Deuschle, U., Meyer, W. K. & Thiesen, H. J. Tetracycline-reversible silencing of eukaryotic promoters. *Mol. Cell Biol.* **15**, 1907–1914 (1995).
- Herchenroder, O., Hahne, J. C., Meyer, W. K., Thiesen, H. J. & Schneider, J. Repression of the human immunodeficiency virus type 1 promoter by the human KRAB domain results in inhibition of virus production. *Biochim. Biophys. Acta* **1445**, 216–223 (1999).
- Rittner, K., Schultz, H., Pavirani, A. & Mehtali, M. Conditional repression of the E2 transcription unit in E1-E3-deleted adenovirus vectors is correlated with a strong reduction in viral DNA replication and late gene expression *in vitro*. *J. Virol.* **71**, 3307–3311 (1997).
- He, H. *et al.* A susceptibility locus for papillary thyroid carcinoma on chromosome 8q24. *Cancer Res.* **69**, 625–631 (2009).
- Ho, T. T. *et al.* Targeting non-coding RNAs with the CRISPR/Cas9 system in human cell lines. *Nucleic Acids Res.* **43**, e17 (2015).
- Nakata, T. & Suzuki, N. Chromogen-based immunohistochemical method for elucidation of the coexpression of two antigens using antibodies from the same species. *J. Histochem. Cytochem.* **60**, 611–619 (2012).
- Nuovo, G. J. *In Situ Molecular Pathology and Co-expression Analyses* (Academic Press, 2013).
- Zhang, S. & Grosse, F. Domain structure of human nuclear DNA helicase II (RNA helicase A). *J. Biol. Chem.* **272**, 11487–11494 (1997).
- Tetsuka, T. *et al.* RNA helicase A interacts with nuclear factor kappaB p65 and functions as a transcriptional coactivator. *Eur. J. Biochem.* **271**, 3741–3751 (2004).
- Schlegel, B. P., Starita, L. M. & Parvin, J. D. Overexpression of a protein fragment of RNA helicase A causes inhibition of endogenous BRCA1 function and defects in ploidy and cytokinesis in mammary epithelial cells. *Oncogene* **22**, 983–991 (2003).
- Jiang, X., Chen, S., Asara, J. M. & Balk, S. P. Phosphoinositide 3-kinase pathway activation in phosphate and tensin homolog (PTEN)-deficient prostate cancer cells is independent of receptor tyrosine kinases and mediated by the p110beta and p110delta catalytic subunits. *J. Biol. Chem.* **285**, 14980–14989 (2010).
- Ueki, K. *et al.* Positive and negative roles of p85 alpha and p85 beta regulatory subunits of phosphoinositide 3-kinase in insulin signaling. *J. Biol. Chem.* **278**, 48453–48466 (2003).
- Gupta, S. C., Singh, R., Pochampally, R., Watabe, K. & Mo, Y. Y. Acidosis promotes invasiveness of breast cancer cells through ROS-AKT-NF-kappaB pathway. *Oncotarget* **5**, 12070–12082 (2014).
- Mayer, B. J. The discovery of modular binding domains: building blocks of cell signalling. *Nat. Rev. Mol. Cell Biol.* **16**, 691–698 (2015).
- Carnero, A. & Paramio, J. M. The PTEN/PI3K/AKT pathway *in vivo*, cancer mouse models. *Front. Oncol.* **4**, 252 (2014).
- Fruman, D. A. & Rommel, C. PI3K and cancer: lessons, challenges and opportunities. *Nat. Rev. Drug Discov.* **13**, 140–156 (2014).
- Worby, C. A. & Dixon, J. E. Pten. *Annu. Rev. Biochem.* **83**, 641–669 (2014).
- Ugi, S. *et al.* Protein phosphatase 2A negatively regulates insulin's metabolic signaling pathway by inhibiting Akt (protein kinase B) activity in 3T3-L1 adipocytes. *Mol. Cell Biol.* **24**, 8778–8789 (2004).

36. Cohen, P., Klumpp, S. & Schelling, D. L. An improved procedure for identifying and quantitating protein phosphatases in mammalian tissues. *FEBS Lett.* **250**, 596–600 (1989).
37. Gao, J. *et al.* Integrative analysis of complex cancer genomics and clinical profiles using the cBioPortal. *Sci. Signal.* **6**, p11 (2013).
38. Cerami, E. *et al.* The cBio cancer genomics portal: an open platform for exploring multidimensional cancer genomics data. *Cancer Discov.* **2**, 401–404 (2012).
39. Reddy, T. R., Tang, H., Xu, W. & Wong-Staal, F. Sam68, RNA helicase A and Tap cooperate in the post-transcriptional regulation of human immunodeficiency virus and type D retroviral mRNA. *Oncogene* **19**, 3570–3575 (2000).
40. Westberg, C., Yang, J. P., Tang, H., Reddy, T. R. & Wong-Staal, F. A novel shuttle protein binds to RNA helicase A and activates the retroviral constitutive transport element. *J. Biol. Chem.* **275**, 21396–21401 (2000).
41. Tang, H. & Wong-Staal, F. Specific interaction between RNA helicase A and Tap, two cellular proteins that bind to the constitutive transport element of type D retrovirus. *J. Biol. Chem.* **275**, 32694–32700 (2000).
42. Stemke-Hale, K. *et al.* An integrative genomic and proteomic analysis of PIK3CA, PTEN, and AKT mutations in breast cancer. *Cancer Res.* **68**, 6084–6091 (2008).
43. Ko, H. R. *et al.* P42 Ebp1 regulates the proteasomal degradation of the p85 regulatory subunit of PI3K by recruiting a chaperone-E3 ligase complex HSP70/CHIP. *Cell Death Dis.* **5**, e1131 (2014).
44. Taniguchi, C. M. *et al.* The phosphoinositide 3-kinase regulatory subunit p85alpha can exert tumor suppressor properties through negative regulation of growth factor signaling. *Cancer Res.* **70**, 5305–5315 (2010).
45. Cizkova, M. *et al.* PIK3R1 underexpression is an independent prognostic marker in breast cancer. *BMC Cancer* **13**, 545 (2013).
46. Cortes, I. *et al.* p85beta phosphoinositide 3-kinase subunit regulates tumor progression. *Proc. Natl Acad. Sci. USA* **109**, 11318–11323 (2012).
47. Li, L., Plummer, S. J., Thompson, C. L., Tucker, T. C. & Casey, G. Association between phosphatidylinositol 3-kinase regulatory subunit p85alpha Met326Ile genetic polymorphism and colon cancer risk. *Clin. Cancer Res.* **14**, 633–637 (2008).
48. Ito, Y., Hart, J. R., Ueno, L. & Vogt, P. K. Oncogenic activity of the regulatory subunit p85beta of phosphatidylinositol 3-kinase (PI3K). *Proc. Natl Acad. Sci. USA* **111**, 16826–16829 (2014).
49. Hanahan, D. & Weinberg, R. A. Hallmarks of cancer: the next generation. *Cell* **144**, 646–674 (2011).
50. Huang, C. H. *et al.* The structure of a human p110alpha/p85alpha complex elucidates the effects of oncogenic PI3Kalpha mutations. *Science* **318**, 1744–1748 (2007).
51. Amzel, L. M. *et al.* Structural comparisons of class I phosphoinositide 3-kinases. *Nat. Rev. Cancer* **8**, 665–669 (2008).
52. Bradford, M. M. A rapid and sensitive method for the quantitation of microgram quantities of protein utilizing the principle of protein-dye binding. *Anal. Biochem.* **72**, 248–254 (1976).
53. Sambrook, J. & Russell, D. W. (eds.). in *Molecular Cloning: A Laboratory Manual*. Ch. 8 Protocol 9, 8.54–8.60 (Cold Spring Harbor Laboratory Press, Cold Spring Harbor, New York, USA, 2001).
54. Montague, T. G., Cruz, J. M., Gagnon, J. A., Church, G. M. & Valen, E. CHOPCHOP: a CRISPR/Cas9 and TALEN web tool for genome editing. *Nucleic Acids Res.* **42**, W401–W407 (2014).
55. Gibson, D. G. *et al.* Enzymatic assembly of DNA molecules up to several hundred kilobases. *Nat. Methods* **6**, 343–345 (2009).
56. Pfaffl, M. W. A new mathematical model for relative quantification in real-time RT-PCR. *Nucleic Acids Res.* **29**, e45 (2001).
57. Si, M. L. *et al.* miR-21-mediated tumor growth. *Oncogene* **26**, 2799–2803 (2007).

Acknowledgements

This work was supported by NIH grant R01 CA154989 (Y.-Y.M.), China Scholarship Council 201408330423 (X.D.) and grant LY15C050002 from the Natural Science Foundation of Zhejiang Province (X.D.).

Author contributions

P.K. conceived the study, performed experiments and wrote the manuscript. J.H. and T.-T.H. performed experiments. F.W. provided reagents and advice on plasmid construction. X.D. conceived the study and wrote the manuscript. Y.M. conceived and supervised the study and wrote the manuscript.

Additional information

Supplementary Information accompanies this paper at <http://www.nature.com/naturecommunications>

Competing financial interests: The authors declare no competing financial interests.

Reprints and permission information is available online at <http://npg.nature.com/reprintsandpermissions/>

How to cite this article: Koirala, P. *et al.* LncRNA AK023948 is a positive regulator of AKT. *Nat. Commun.* **8**, 14422 doi: 10.1038/ncomms14422 (2017).

Publisher's note: Springer Nature remains neutral with regard to jurisdictional claims in published maps and institutional affiliations.



This work is licensed under a Creative Commons Attribution 4.0 International License. The images or other third party material in this article are included in the article's Creative Commons license, unless indicated otherwise in the credit line; if the material is not included under the Creative Commons license, users will need to obtain permission from the license holder to reproduce the material. To view a copy of this license, visit <http://creativecommons.org/licenses/by/4.0/>

© The Author(s) 2017